⌘ *Author's Choice*

THE JOURNAL OF BIOLOGICAL CHEMISTRY VOL. 285, NO. 6, pp. 3825–3832, February 5, 2010

Global Consequences of Activation Loop Phosphorylation on Protein Kinase A*[S]

Received for publication, September 1, 2009, and in revised form, December 3, 2009 Published, JBC Papers in Press, December 4, 2009, DOI 10.1074/jbc.M109.061820

Jon M. Steichen[‡1], Ganesh H. Iyer[‡1,2], Sheng Li[§], S. Adrian Saldanha[‡3], Michael S. Deal[‡], Virgil L. Woods, Jr.[§], and Susan S. Taylor[‡¶‖4]

From the Departments of [‡]Chemistry and Biochemistry and [¶]Pharmacology, the [‖]Howard Hughes Medical Institute, and the [§]Department of Medicine and Biomedical Sciences Graduate Program, University of California, San Diego, La Jolla, California 92093

Phosphorylation of the activation loop is one of the most common mechanisms for regulating protein kinase activity. The catalytic subunit of cAMP-dependent protein kinase autophosphorylates Thr^{197} in the activation loop when expressed in *Escherichia coli*. Although mutation of Arg^{194} to Ala prevents autophosphorylation, phosphorylation of Thr^{197} can still be achieved by a heterologous protein kinase, phosphoinositide-dependent protein kinase (PDK1), *in vitro*. In this study, we examined the structural and functional consequences of adding a single phosphate to the activation loop of cAMP-dependent protein kinase by comparing the wild type C-subunit to the R194A mutant either in the presence or the absence of activation loop phosphorylation. Phosphorylation of Thr^{197} decreased the K_m by ~15- and 7-fold for kemptide and ATP, respectively, increased the stability of the enzyme as measured by fluorescence and circular dichroism, and enhanced the binding between the C-subunit and IP20, a protein kinase inhibitor peptide. Additionally, deuterium exchange coupled to mass spectrometry was used to compare the structural dynamics of these proteins. All of the regions of the C-subunit analyzed underwent amide hydrogen exchange at a higher or equal rate in the unphosphorylated enzyme compared with the phosphorylated enzyme. The largest changes occurred at the C terminus of the activation segment in the $p + 1$ loop/APE regions and the αH-αI loop motifs and leads to the prediction of a coordinated phosphorylation-induced salt bridge between two conserved residues, Glu^{208} and Arg^{280}.

The protein kinase superfamily is one of the largest in the human genome and one of the most relevant to disease, and the protein kinases serve as major on/off switches for almost every pathway in the cell. However, most protein kinases are themselves also regulated by a strategic phosphate. Kinases are typically expressed in an inactive state and converted into a fully active form by the addition of a phosphate to the activation loop (1). Here we address the global importance of this one activation loop phosphate.

cAMP-dependent protein kinase (PKA)[5] is one of the best understood members of the protein kinase superfamily and has served as a prototype in many ways. It belongs to the AGC group of protein kinases, and in addition to the general features it shares with all protein kinases, it shares many features unique to the AGC group including a conserved C-terminal tail (2). In PKA, as with many kinases, phosphorylation of a threonine residue in the activation loop (Thr^{197}) converts the enzyme from an inactive to an active state. The activation loop phosphate on Thr^{197} coordinates the active site by bridging the C-helix (His^{87}), the catalytic loop (Arg^{165}), β9 (Lys^{189}), and the activation loop (Thr^{195}) (see Fig. 1). As a general rule, kinases that require phosphorylation of their activation loop contain an arginine preceding the catalytic aspartate (Asp^{166} in PKA) (3). Additionally, the DFG motif (residues 184–186) has been shown to be highly dynamic in many kinases and important for activation by coordinating Mg^{2+} at the active site, as well as for stabilizing the C-helix through a hydrophobic spine (4–7). Lastly, there is a conserved APE motif (residues 206–208) at the C-terminal end of the activation segment. The function of this conserved region has not been well characterized.

Early studies showed qualitatively that Thr^{197} phosphorylation was important for binding to protein kinase inhibitor (PKI) (8), and in yeast the C-subunit was shown to be defective in binding the R-subunit when the activation loop was not phosphorylated (9). A kinetic study of a T197A mutant demonstrated the significance of having a phosphate on the activation loop (10). In a separate study, analysis of a kinase dead mutant of PKA (K72H) showed long range effects on the structure using hydrogen/deuterium exchange coupled with mass spectrometry (H/DMS) (11). However, the K72H mutation prevented phosphorylation in both the activation loop as well as

* This work was supported, in whole or in part, by National Institutes of Health Grants GM19301 (to S. S. T.) and CA099835, CA118595, AI076961, AI081982, AI2008031, AI072106, AI068730, GM037684, GM020501, and GM066170 (to V. L. W.). This work was also supported by National Institutes of Health Pharmacological Sciences Training Grant GM007752 (to J. M. S.) and by Discovery Grant UC10591 from the University of California IUCRP Program, BiogenIdec corporate sponsor (to V. L. W.).

⌘ *Author's Choice*—Final version full access.

[S] The on-line version of this article (available at http://www.jbc.org) contains supplemental Figs. S1–S3.

[1] Both authors contributed equally to this work.

[2] Present address: Vertex Pharmaceuticals Incorporated, Cambridge, MA 02139.

[3] Present address: The Scripps Research Institute, Scripps Florida, 130 Scripps Way #1A1, Jupiter, FL 33458.

[4] To whom correspondence should be addressed: Dept. of Chemistry and Biochemistry, University of California, San Diego, 9500 Gilman Dr., La Jolla, CA 92093. Tel.: 858-534-8190; Fax: 858-534-8193; E-mail: staylor@ucsd.edu.

[5] The abbreviations used are: PKA, cAMP-dependent protein kinase; PDK1, phosphoinositide-dependent protein kinase; H/DMS, hydrogen/deuterium exchange coupled to mass spectrometry; PKI, protein kinase inhibitor; PKC, protein kinase C; MOPS, 4-morpholinepropanesulfonic acid; WT, wild type; MAP, mitogen-activated protein.

the turn motif, such that the effects of phosphorylation could not be isolated from the effects of the lysine mutation.

The effects of activation loop phosphorylation in other AGC kinases have also been studied both biochemically (12–15) and structurally (15–18). These studies demonstrated a surprising amount of variation among very similar kinases. For the conventional protein kinase C isoenzyme, PKCβII, activation loop phosphorylation plays a crucial role in the catalytic activity of the enzyme (12), whereas for the novel isoenzyme, PKCδ, phosphorylation does not appear to be important for catalytic activity (13, 14). There is also structural variation. In the absence of phosphorylation, the C-helix of PDK1 remains in an active conformation (15), whereas in Akt2, the C-helix is almost completely disordered (16). GRK2, on the other hand, does not contain the conserved Ser/Thr on the activation loop and thus does not require phosphorylation for activity (17). The majority of these studies have been carried out by mutating the phosphorylation site to an alanine residue. The challenge is to develop an easily reversible system where one can compare the same protein in its phosphorylated state and in its dephosphorylated state.

PKA, like many kinases, is complicated further because there are two phosphorylation sites: Thr^{197} on the activation loop and Ser^{338} in the turn motif. In bacteria, Thr^{197} is autophosphorylated by another C-subunit molecule (*trans*-phosphorylation), whereas Ser^{338} is autophosphorylated by an intramolecular (*cis*) mechanism following phosphorylation of the activation loop (19). In mammalian cells, PKA is likely phosphorylated by PDK1 or a PDK1-like enzyme (20, 21). All of the structures of PKA to date correspond to the fully phosphorylated enzyme. In some cases the enzyme is inactive because it is bound to an inhibitor.

To study the functional consequences of a single phosphate on the activation loop of the PKA C-subunit, we replaced an arginine residue in the activation loop with an alanine (R194A). This P-3 arginine is required for PKA substrate recognition (see Fig. 1). Arg^{194} does not have any known function but allows PKA to autophosphorylate Thr^{197} when expressed at high levels in *Escherichia coli*. After Arg^{194} is replaced with alanine, Thr^{197} is no longer autophosphorylated. The R194A mutant is stable for expression in bacteria, and Thr^{197} can be readily phosphorylated by PDK1 *in vitro*. Here, we demonstrate that Ser^{338} is still autophosphorylated in the R194A mutant. Thus, we are able to purify an inactive form of the C-subunit that can be converted readily into a fully active enzyme by PDK1. This mutant protein provides a good experimental model to precisely quantify the effects of adding a single phosphate to PKA. By comparing the catalytic efficiency, stability, and interaction with an inhibitor, we found that all of the regions of the protein are profoundly affected. These conclusions were confirmed by using H/DMS to map solvent-accessible sites. Both N-lobe (residues 1–126) and active site peptides showed enhanced deuteration. Most striking, however, was the complete exposure of the region surrounding the APE motif (residues 199–211) at the end of activation loop; this same region is well protected in the fully phosphorylated enzyme. In all cases the properties of the unphosphorylated R194A protein reverted to those of the wild type protein following phosphorylation by PDK1. This is the first demonstration showing that the addition of a single phosphate can have such a profound and global effect on the structure and function of protein kinase A. It also suggests that phosphorylation of the activation loop may be linked in PKA to an "APE-flip" mechanism.

EXPERIMENTAL PROCEDURES

Materials—The reagents used were the pET15b expression vector (Invitrogen), *E. coli* strains BL21(DE3) (Novagen, Madison, WI), QuikChange mutagenesis kit (Stratagene), horseradish peroxidase-conjugated anti-rabbit IgG (Amersham Biosciences), SuperSignal West Pico Chemiluminiscent substrate detection kit (Pierce), and oligonucleotides (Sigma). Antibodies against the catalytic subunit of PKA and the Ser^{338} phosphorylation site were described previously (19), whereas antibodies that specifically recognize the phosphorylated activation loop of PKC, referred to as α-$Thr(P)^{197}$, were a gift from A. Newton (University of California, San Diego). DNA sequencing was performed with the ABI PRISM 310 genetic analyzer from PerkinElmer Life Sciences. All other materials were reagent grade from standard commercial sources.

Expression and Purification of the PKA Catalytic Subunit Mutants—His_6-tagged R194A mutants in pET15b vector (amp^r) were expressed in *E. coli* (BL21 (DE3)). Mid-exponential cultures of BL21 cells were induced with 0.5 mM isopropyl β-D-thiogalactopyranoside and grown for another 12 h at 16 °C prior to harvesting at 6000 rpm. Following resuspension in lysis buffer (50 mM KH_2PO_4, 20 mM Tris-HCl, 100 mM NaCl, 5 mM β-mercaptoethanol, pH 8.0), the cells were lysed using a Microfluidizer (Microfluidics) at 18,000 p.s.i. The cells were clarified by centrifugation at 17,000 rpm at 4 °C in a Beckman JA20 rotor for 50 min, and the supernatant was incubated with ProBond Resin (Invitrogen) and pre-equilibrated in the same buffer for 1 h at 4 °C. The resin was then spun down at 3000 rpm, and the supernatant was removed. Two washes with the lysis buffer were followed by two washes with wash buffer (50 mM KH_2PO_4, 20 mM Tris-HCl, 100 mM or 1 M NaCl, 10 mM imidazole, and 5 mM β-mercaptoethanol, pH 7). An imidazole elution buffer using four different concentrations of imidazole (50, 100, 200, and 500 mM) in wash buffer was used to elute the His-tagged protein. Samples containing the most protein were loaded onto a prepacked Mono-S 10/10 (GE Healthcare) cation exchange column equilibrated in 20 mM KH_2PO_4, 20 mM KCl, and 2.5 mM dithiothreitol, pH 7.15, and then eluted with equilibration buffer containing a KCl gradient ranging from 0 to 1 M. To obtain the phosphorylated form of R194A, the cells were co-expressed with PDK1 enzyme cloned in PGEX and Thr^{197}-phosphorylated R194A (pR194A) was purified using the same approach as R194A.

Urea Unfolding and Fluorescence Measurements—Amberlite MB-150 (Sigma) mixed bed exchanger was added to 8.0 M urea solution and stirred for 1 h to remove ionic urea degradation products. The urea solution was filtered and frozen at −20 °C. Proteins (0.12 mg/ml) were unfolded in various concentrations of urea ranging from 0 to 6 M for 0.5 h at room temperature and monitored by steady-state fluorescence. Fractional unfolding curves were constructed assuming a two-state model and using $F_U = 1 - [(R - R_U)/(R_F - R_U)]$, where F_U is the fraction of the

unfolded protein, R is the fluorescence measurement, and R_F and R_U represent the values of R for the folded and unfolded states, respectively (22). For unfolding monitored by fluorescence, R is the observed ratio of intensity at 356/334 nm with excitation at 295 nm.

Circular Dichroism—Thermal unfolding measured by circular dichroism was carried out as described previously (11).

Kinetic Assay—Enzymatic activity was measured spectrophotometrically as described previously (23). The K_m values for ATP and peptide substrate were determined using Michaelis-Menten kinetics. 75 nM C-subunit was pre-equilibrated in 50 mM MOPS buffer, pH 7.0, containing 1 mM ATP, 10 mM $MgCl_2$, 1 mM phosphoenolpyruvate, 0.3 mM NADH, lactate dehydrogenase (12 units), and pyruvate kinase (4 units) in a final volume of 100 μl. The reactions were initiated by adding various amounts of Kemptide (LRRASLG). All of the measurements were made in triplicate. The K_m and V_{max} were determined from a Hanes-Woolf plot.

Synthesis of FLU-IP20—To form N-terminal fluorescently tagged IP20, 900 μM of IP20 (PKI_{5-24}) and 9 mM of 5-(and-6)-carboxyfluorescein (Molecular Probes) in 100 mM sodium phosphate, pH 7.4, were mixed overnight at 4 °C. Labeled IP20 was purified by high pressure liquid chromatography with a 20–60% acetonitrile gradient containing 0.1% trifluoroacetic acid on a C18 reverse phase column (Vydac). The mass of the labeled peptide was verified by mass spectrometry on a Voyager DE-STR matrix-assisted laser desorption ionization time-of-flight (Applied Biosystems).

Characterization of FLU-IP20 Binding by Fluorescence Polarization—Fluorescence polarization experiments were performed at 25 °C in a Costar 96-well solid black microplate (Corning) with a GeniosPRO microplate reader (Tecan). To determine the apparent K_d for FLU-IP20, serial dilutions of PKA or PKA mutants were made in assay buffer containing 25 mM HEPES, pH 7.4, 0.002% Triton X-100, 8 mM $MgCl_2$, and 250 μM or 2 mM ATP. To these solutions was added FLU-IP20 to a final concentration of 1 nM, and the binding reaction was incubated for 30 min at 25 °C in the dark. Readings were taken after 30 min, because no change in polarization was observed after 15 min, indicating that the binding reaction had reached equilibrium. The samples were excited at 485 nm, and emission in the parallel and perpendicular directions was detected at 535 nm. The polarization value measured for each sample was based on the average of 10 reads each with a 40-μs integration time. The data sets were fit to a sigmoidal dose response by nonlinear regression with GraphPad Prism (San Diego, CA).

H/DMS Analysis—Deuterium exchange analysis of the catalytic subunit was carried out as described previously (24) with the following changes. The wild type and R194A mutant C-subunits were at 2.5 mg/ml final concentration in the deuterium exchange buffer. Back exchange was estimated to be 20% based on comparison with previously published analysis of the C-subunit (11, 24).

RESULTS

Purification and Phosphorylation State of R194A—To evaluate the importance of the activation loop phosphate, we expressed and purified a mutant form of the PKA catalytic subunit that cannot be autophosphorylated as was described previously (25). The consensus sequence for PKA substrates is shown in Fig. 1. Because the P-3 arginine is required for PKA substrate recognition, the R194A mutation makes it defective in autophosphorylation.

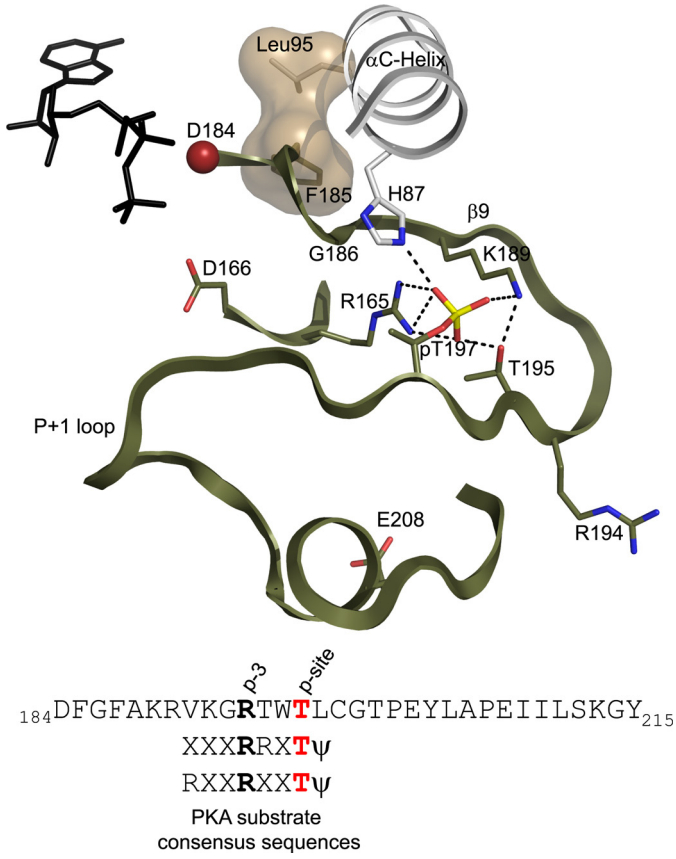

FIGURE 1. **Interactions of the activation loop phosphate in the C-subunit and other conserved regions of the activation segment.** The activation segment is colored *olive* with the sequence shown below the structure along with two common consensus sequences of PKA substrates. Phe^{185} and Leu^{95} are part of the hydrophobic regulatory spine (4) and are shown as a *tan* molecular surface. ATP is colored *black*. The P-3 site and position of Arg^{194} are in *bold*, and the P-site is colored *red*.

Our first step was to evaluate the phosphorylation state of the R194A mutant using phospho-specific antibodies. We confirmed that the purified protein was not phosphorylated on Thr^{197} (Fig. 2). The enzyme, however, was not defective in its ability to autophosphorylate Ser^{338}. Thus, the only difference between this mutant and the wild type catalytic subunit is a single phosphate on Thr^{197}. *In vitro*, PDK1, but not wild type C-subunit, was able to phosphorylate the R194A mutant.

The Addition of Phosphate to the Activation Loop Increases the Catalytic Efficiency of PKA—The kinetic effects of adding phosphate to the PKA activation loop were measured for the first time without mutating the phosphorylation residue Thr^{197}. In Table 1, the steady-state kinetics of the unphosphorylated mutant is compared with the wild type C-subunit. In the unphosphorylated state there were 15- and 7-fold increases in the K_m for kemptide and ATP, respectively, compared with the phosphorylated state. The k_{cat}, however, was not significantly affected by phosphorylation. Following the phosphorylation of R194A by PDK1, the steady-state kinetic parameters were

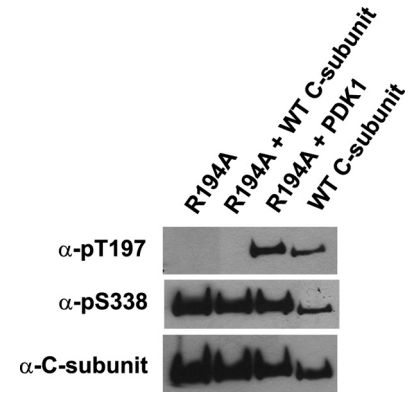

FIGURE 2. **Phosphorylation state of R194A mutants.** R194A mutants, with and without treatment by PDK1 or wild type C-subunit, were probed with α-Thr(P)[197], α-Ser(P)[338], and α-C-subunit antibody.

TABLE 1

Comparison of steady-state kinetic parameters for WT C-subunit and pR194A and R194A mutants measured on kemptide by the method of Cook *et al.* (23)

C-subunit	k_{cat}	K_m		k_{cat}/K_m (Kemp)
		Kemp	ATP	
	s^{-1}	μM	μM	
WT	21 ± 1	26 ± 7	38 ± 5	0.8
pR194A	16 ± 1	27 ± 4	36 ± 6	0.6
R194A	22 ± 3	410 ± 30	275 ± 6	0.05

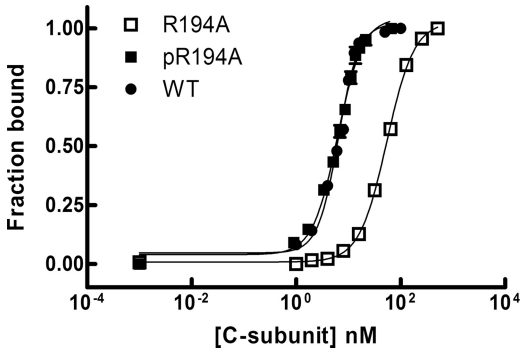

FIGURE 3. **Fluorescence polarization of FLU-IP20 binding to the C-subunit.** Titration of WT and mutant C-subunits (R194A and pR194A) was at fixed concentrations of ATP and fluorescently labeled IP20. The values are the means ± S.E., $n = 3$ for R194A and pR194A and $n = 2$ for WT.

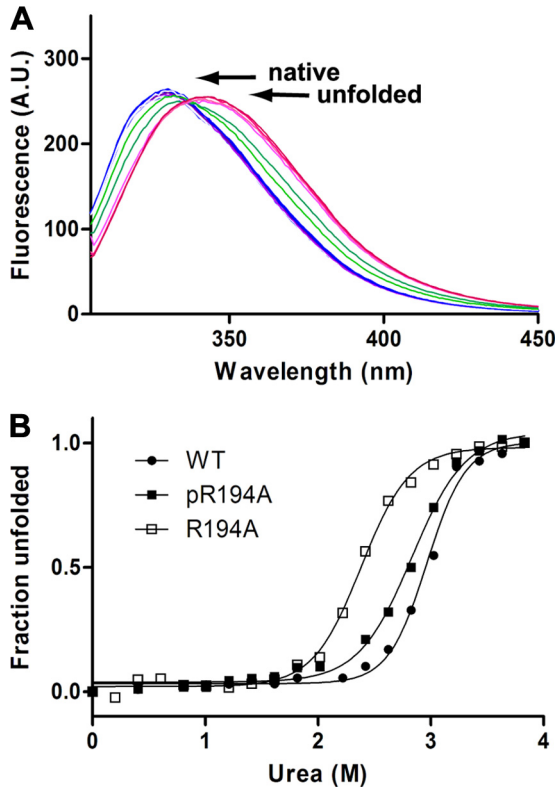

FIGURE 4. **Urea-induced unfolding profiles.** *A*, tryptophan fluorescence of the Wild type C-subunit is shown at varying concentrations of urea. *B*, comparison of the urea denaturation curves for WT, R194A, and pR194A C-subunit. The fraction of protein unfolded is shown as a function of urea concentration monitored by intrinsic tryptophan fluorescence.

TABLE 2

Thermal denaturation (T_m (°C)) as an indicator of protein stability measured by CD spectroscopy

Ligand	Apo	ATP	H89
WT	46.9	52.5	54.2
pR194A	46.5	51.3	53.3
R194A	41.3	44.8	47.1

nearly identical to the wild type C-subunit, confirming that the arginine mutation itself does not play a role in catalysis.

There Is a Decreased Affinity for the Physiological Inhibitor PKI without Phosphate on the Activation Loop—To evaluate the effect of activation loop phosphorylation on interaction with an inhibitor of PKA, we utilized the heat-stable PKI. To measure interactions between the C-subunit and PKI, we labeled a 20-amino acid peptide, corresponding to residues 5–25 of PKI (IP20) with fluorescein and used fluorescence anisotropy to measure its affinity for the different C-subunits. The presence of a phosphate resulted in a 9-fold increase in affinity between the C-subunit and IP20 (Fig. 3). The EC_{50} was 6.4 and 6.2 nM for the wild type and pR194A, respectively, and 54 nM for the R194A.

Phosphorylation Increases the Stability of the Catalytic Subunit—The unfolding of the C-subunit was measured by monitoring the intrinsic tryptophan fluorescence from 300–450 nm (excitation at 295 nm) with increasing urea concentration. There is a ~15-nm shift in λ_{max} when the C-subunit is unfolded in urea (Fig. 4*A*). The wild type C-subunit had a transition point of 3 M urea compared with 2.8 M for pR194A and 2.4 M for R194A (Fig. 4*B*). We also used circular dichroism to evaluate the global conformational state in the presence and the absence of ligands. Both Mg/ATP and H89 increased the thermostability of the C-subunit with or without phosphate; however, the unphosphorylated enzyme (R194A) was less stable than the phosphorylated enzymes (WT and pR194A) in each case (Table 2).

Deuterium Exchange Shows That the Small Lobe of the Catalytic Subunit Is More Solvent-exposed without Thr[197] Phosphorylation—To resolve structural and dynamic changes that occur as a result of Thr[197] phosphorylation, we used H/DMS. The results showed that the presence of the phosphate was sensed in the small lobe, in the active site cleft, and in the large lobe (see supplemental Fig. S1 for peptide coverage map and supplemental Fig. S2 for complete H/DMS analysis). Nearly all of the peptides in the small lobe showed an increase in solvent accessibility in the R194A mutant, whereas the pR194A mutant was nearly identical to WT. The Gly-rich loop (residues 41–54) is a good indicator of the conformational state of the

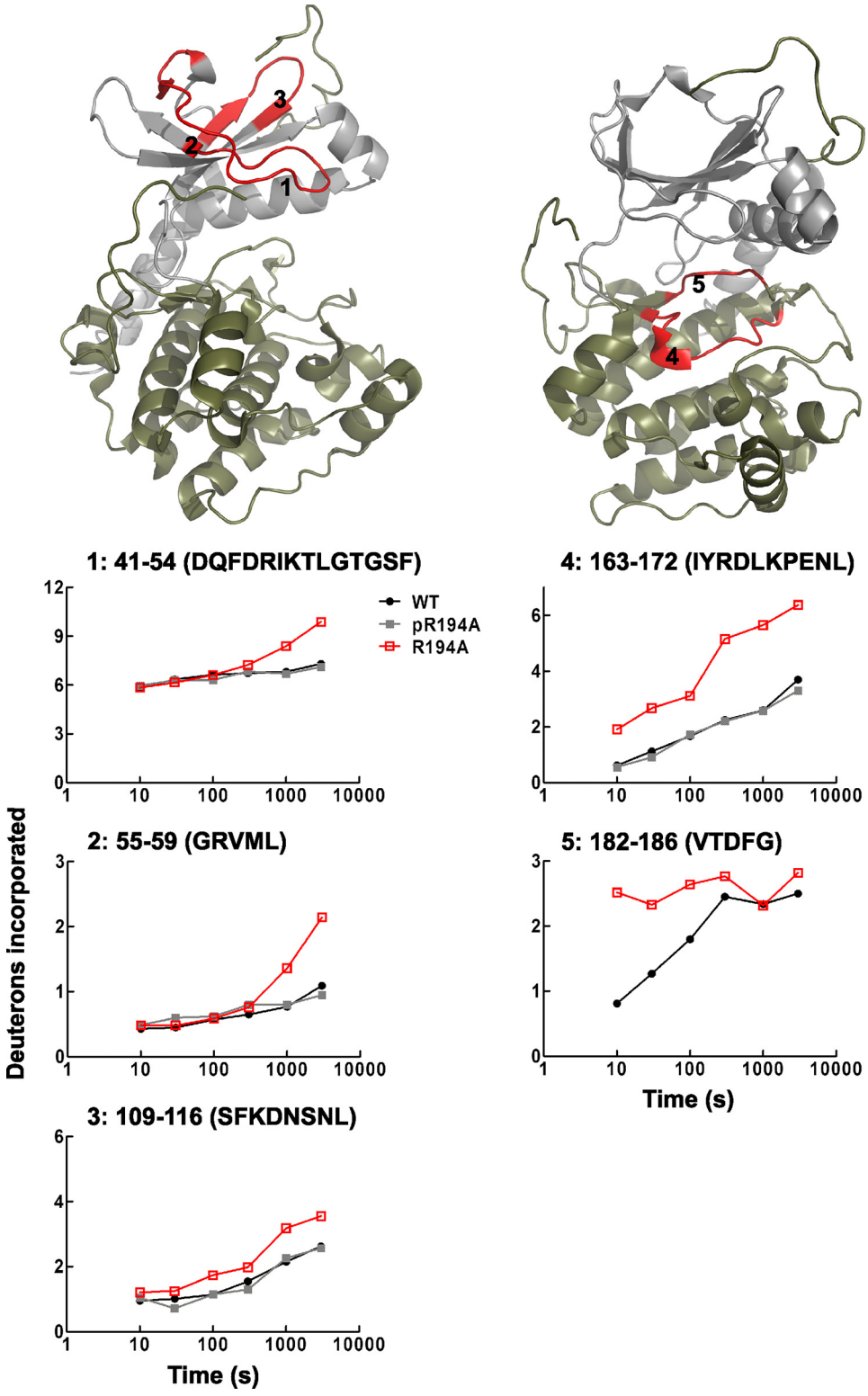

FIGURE 5. **H/DMS data for peptides with increased rate of deuterium exchange in the unphosphorylated mutant.** Time course for deuterium exchange in the small lobe with peptides 1 (residues 41–54), 2 (residues 55–59), and 3 (residues 109–116) and in the active site region, peptides 4 (residues 163–172) and 5 (residues 182–186) shown in *red*. The scale of the *y* axis is the maximum number of exchangeable amides. The large lobe of the C-subunit (residues 127–350) is colored *olive*, and the small lobe (residues 1–126) is colored *gray* for reference.

small lobe. Three peptides, including the Gly-rich Loop, identified in all three proteins are mapped onto the PKA structure in its apo conformation (26) in Fig. 5. The solvent accessibility of each peptide was reduced to wild type levels when the mutant protein was phosphorylated by PDK1.

The Dynamics of the Active Site Are Strongly Dependent on the Phosphorylation State of the Activation Loop—The DFG motif (residues 184–186) is an indicator of the activation state of the enzyme for many protein kinases (4–7). The catalytic loop is another critical part of the active site and specifically bridges the activation loop phosphate with the catalytic base. The DFG peptide (residues 182–186) showed rapid deuterium exchange (<10 s) in the unphosphorylated state, but exchange was slowed to 5 min in the phosphorylated state (Fig. 5 and supplemental Fig. S3). The catalytic loop peptide (residues 163–172) showed an increase in solvent accessibility, exchanging five deuterons in the unphosphorylated state and only three deuterons in the phosphorylated state after 50 min in deuterium.

Phosphorylation Links the Activation Loop to the αH-αI Loop—The largest changes in solvent accessibility occur near the end of the activation segment in the $p + 1$ loop/APE motif (199–211) and the αH-αI loop (278–296) peptides (Fig. 6), which are linked through a salt bridge (Glu^{208}/Arg^{280}). In the 199–211 peptide, the phosphorylated enzyme is well protected from solvent up to 50 min in deuterium, whereas the unphosphorylated enzyme exchanges roughly all of its amide hydrogens after only 5 min in deuterium. The 278–296 peptide exchanged four deuterons more in the unphosphorylated protein than in the phosphorylated protein after 30 s in deuterium.

Hydrophobic Core—Although much of the molecule shows increased solvent accessibility in the unphosphorylated state, there remains a solid helical core that does not exchange deuterons with the solvent (Fig. 7). The αE and αF helices are buried within the core of the C-subunit, whereas the αC, αH, and αJ helices, although exposed to the solvent, show equally slow rates of deuterium exchange.

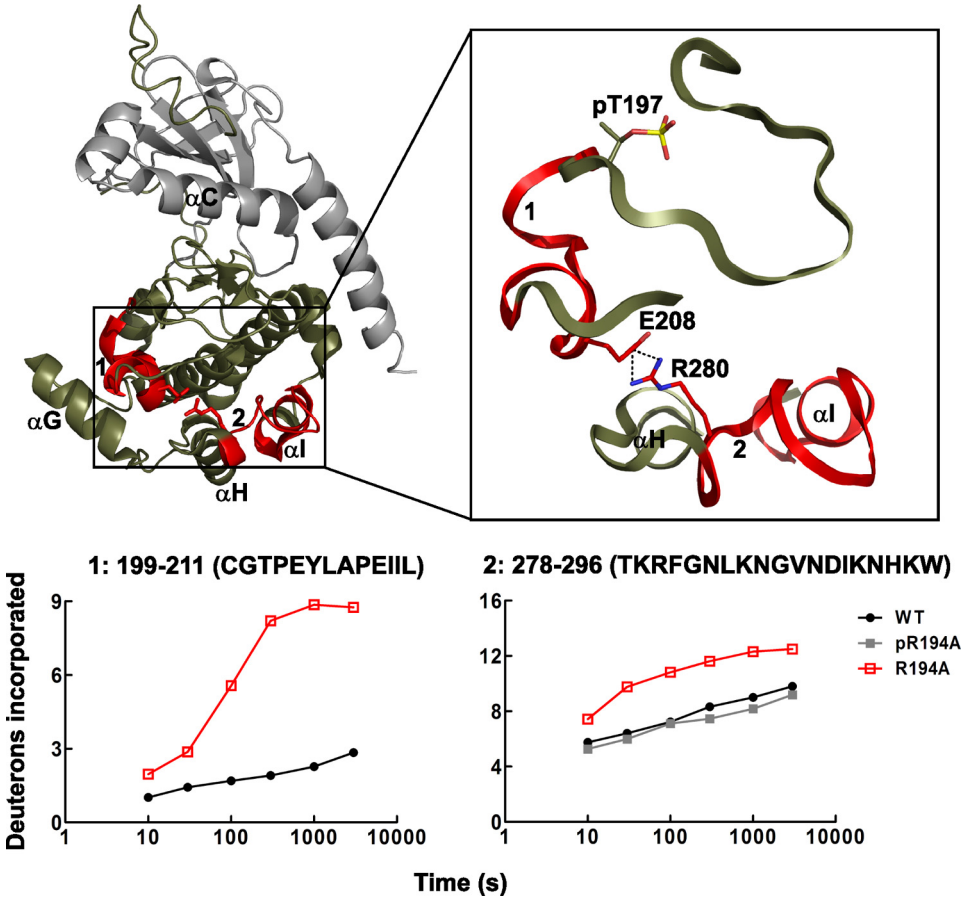

FIGURE 6. **Deuterium exchange in the activation segment and the αH-αI loop.** Time course for deuterium exchange in the large lobe with peptides 1 (residues 199–211) and 2 (residues 278–296) colored in *red*. The scale of the *y* axis is the maximum number of exchangeable amides. The large lobe of the C-subunit (residues 127–350) is colored *olive*, and the small lobe (residues 1–126) is colored *gray* for reference.

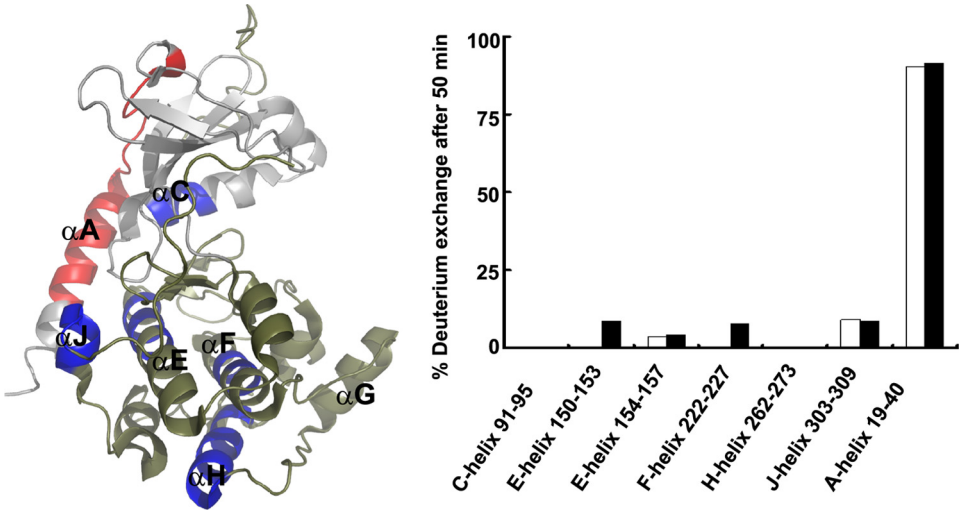

FIGURE 7. **Stable helical core of the PKA catalytic subunit.** The percentages of deuterium exchange after 50 min in deuterium in peptides from helices C, E, F, H, and J are shown. WT (*white bars*) and R194A (*black bars*). Helical peptides that exchanged less than 10% of their amide hydrogens are mapped onto the structure of the C-subunit and colored *blue*. The A-Helix is a fast exchanging helix and is shown in *red*. Where bars are not shown, no exchange was observed. The large lobe (residues 127–350) is colored *olive*, and the small lobe (residues 1–126) is colored *gray*.

DISCUSSION

Almost every protein kinase is regulated by phosphorylation of its activation loop. The PKA C-subunit is phosphorylated rapidly and constitutively in mammalian cells by a PKA kinase, most likely a PDK1-like kinase (20, 21). The phosphorylated catalytic subunit is then regulated by four R-subunit isoforms that are in turn controlled by the second messenger, cAMP. This is in contrast to other kinases such as MAP kinases and protein-tyrosine kinases that are controlled by dynamic and transient activation loop phosphorylation and dephosphorylation. Other AGC kinases, such as PKC, are also regulated by second messengers. The activation loop phosphate of PKA is resistant to phosphatases which is, in part, due to its close proximity to a cysteine residue in the activation loop (27).

The effects of activation loop phosphorylation have not been well studied in the AGC kinases without mutating the phosphorylated residue. The results shown here demonstrate for the first time the consequences that result from adding a single phosphate to the activation loop of the PKA catalytic subunit. Previous attempts to study the effects of activation loop phosphorylation have generally been carried out by replacing the phosphorylation site with either an alanine for Ser/Thr protein kinases or a phenylalanine for tyrosine protein kinases. Here, we generated a mutant form of the catalytic subunit that does not autophosphorylate Thr^{197}, which we were then able to phosphorylate by co-expression with PDK1. This study demonstrates the feasibility of utilizing the R194A mutation as a model system for studying the effects of PKA activation loop phosphorylation. The phosphorylated mutant (pR194A) is similar to the wild type enzyme in stability, catalytic efficiency, ability to bind IP20, and solvent accessibility. There was a measurable difference in every property that was tested when comparing the C-subunit in the presence and absence of phosphorylation, including enhanced binding to a physiological inhibitor, increased thermodynamic stability, and a ~15-fold increase in catalytic efficiency. Additionally, there were many regions throughout the protein that showed

increased solvent accessibility in the unphosphorylated enzyme, most significantly in the $p + 1$ loop/APE region.

In the case of PKA, a mutation of the phosphorylated residue (Thr^{197}) to an alanine had a much more severe effect on the catalytic activity (10). The T197A mutant had a catalytic efficiency that was ~500-fold worse than the wild type C-subunit compared with ~15-fold for the R194A mutant. This indicates that the hydroxyl group of the threonine residue may play a significant role in stabilizing the active site, and mutating the phosphorylation site to alanine may not be an appropriate method for studying the effects of activation loop phosphorylation. Thus, our goal was to quantify the effects of activation loop phosphorylation without mutating the phosphorylation residue. It was also shown previously and qualitatively that activation loop phosphorylation enhances binding to PKI (8). Here we demonstrate quantitatively that there is a ~10-fold increase in affinity between the C-subunit and IP20 when the activation loop is phosphorylated.

Moore *et al.* (25), previously found that the E208A mutant in the APE motif blocked PDK1-mediated phosphorylation but did not block autophosphorylation. The structure of PKA in its active state showed that Glu^{208} is completely buried, making it difficult to explain how a mutation of E208A could block phosphorylation by another kinase. Additionally, Torkamani *et al.* (28) recently identified a conserved ion pair (Glu^{208}/Arg^{280} in PKA) as a disease "hot spot" in a number of protein kinases. Our H/DMS analysis shows that this APE region (peptide 199–211) is very well protected from solvent in the phosphorylated enzyme but exchanges all of its amide hydrogens with the solvent in the unphosphorylated state within 5 min. Several recently solved crystal structures from diverse protein kinases (including checkpoint kinase 2, Ste20-like kinase, lymphocyte-originated kinase, and death-associated protein kinase 3) (29–32) have revealed that the $p + 1$ loop/APE motif has the capacity to undergo large conformational changes. Our deuterium exchange analysis is the first indication that the $p + 1$ loop/APE motif from an AGC kinase is a highly dynamic region that may undergo large conformational changes in the absence of activation loop phosphorylation. This conformational change may make the activation loop more accessible so that phosphorylation by another kinase, such as PDK1, can occur.

H/DMS has been used previously to analyze the C-subunit of PKA, and several mutations were found to increase the solvent accessibility of the αH-αI loop (11, 24). Residues 282–286 form a loop that is specific to the AGC kinases (2). Our data also show that the αH-αI loop becomes more solvent-exposed in the unphosphorylated enzyme, and we propose that this is a consequence of the APE conformational change. The only direct interaction between the activation segment and the αH-αI loop is through a salt bridge formed between Glu^{208} in the APE motif and Arg^{280} in the αH-αI loop. It is likely that Thr^{197} phosphorylation stabilizes this Glu^{208}/Arg^{280} salt bridge. This ion pair is conserved in all protein kinases with the exception of the casein kinases. H/DMS has also been used to study two other protein kinases, extracellular signal-regulated kinase 2 (ERK2) and p38 MAP kinase, in the presence and absence of activation loop phosphorylation (33, 34). Neither protein showed a large change in solvent accessibility in the region around the APE motif (a one- or two-deuteron difference), and correspondingly, there was relatively little change in the αH-αI loop peptide. Thus, the solvent accessibility changes in the APE and αH-αI loop regions may be more pronounced in PKA and in other AGC kinases that have a unique and conserved insert in the αH-αI loop.

The deuterium exchange analysis also revealed several helices that do not exchange amide hydrogens with the solvent. The αE and αF helices are buried within the hydrophobic core of the protein, whereas the αC, αH, and αJ helices are at the surface of the enzyme where they are partially exposed to solvent. Nevertheless, many of the backbone amides within these helices appear to form highly stable hydrogen bonds to the backbone carbonyl oxygens, which prevents any deuterium exchange from occurring. In contrast, the αA helix exchanges 90% of its amide hydrogens by 50 min in deuterium. These data also indicate that the loss of stability in the unphosphorylated mutant is not due to a change in the hydrophobic core of the protein. More likely, it is the dynamic change in the loop regions, in particular the $p + 1$ loop/APE motif and the αH-αI loop, that decreases the stability. The effect on stability was not as severe as that seen with the K72H mutant, which, in addition to the lysine mutation, was lacking both Thr^{197} and Ser^{338} phosphorylation (11).

In conclusion, we have made a biophysical comparison of two physiological states of the PKA catalytic subunit and have identified several novel properties associated with activation loop phosphorylation. Based on our kinetic analysis, the Thr^{197} hydroxyl group may be important for stabilizing the active site in the absence of phosphorylation because it is more active than simply replacing the threonine with alanine. More importantly, whereas the core of the protein remains stable in the absence of phosphorylation, the loop regions are highly dynamic. Most significantly, the dynamics of the APE motif and αH-αI loop, two regions that are linked by a conserved ion pair and are known to be associated with many diseases, are strongly dependent on the phosphorylation state of the activation loop.

Acknowledgments—We thank Daniel Alyeshmari and Drs. Jie Yang and Chris Eggers for helpful discussions and technical assistance and Drs. Alexandr Kornev and Cecilia Cheng for critical reading of the manuscript and for some of the figure preparation.

REFERENCES

1. Nolen, B., Taylor, S., and Ghosh, G. (2004) *Mol. Cell* **15,** 661–675
2. Kannan, N., Haste, N., Taylor, S. S., and Neuwald, A. F. (2007) *Proc. Natl. Acad. Sci. U.S.A.* **104,** 1272–1277
3. Johnson, L. N., and Lewis, R. J. (2001) *Chem. Rev.* **101,** 2209–2242
4. Kornev, A. P., Haste, N. M., Taylor, S. S., and Eyck, L. F. (2006) *Proc. Natl. Acad. Sci. U.S.A.* **103,** 17783–17788
5. Levinson, N. M., Kuchment, O., Shen, K., Young, M. A., Koldobskiy, M., Karplus, M., Cole, P. A., and Kuriyan, J. (2006) *PLoS Biol.* **4,** e144
6. Vogtherr, M., Saxena, K., Hoelder, S., Grimme, S., Betz, M., Schieborr, U., Pescatore, B., Robin, M., Delarbre, L., Langer, T., Wendt, K. U., and Schwalbe, H. (2006) *Angew. Chem. Int. Ed Engl.* **45,** 993–997
7. Kannan, N., and Neuwald, A. F. (2005) *J. Mol. Biol.* **351,** 956–972
8. Steinberg, R. A., Cauthron, R. D., Symcox, M. M., and Shuntoh, H. (1993) *Mol. Cell Biol.* **13,** 2332–2341
9. Levin, L. R., and Zoller, M. J. (1990) *Mol. Cell Biol.* **10,** 1066–1075
10. Adams, J. A., McGlone, M. L., Gibson, R., and Taylor, S. S. (1995) *Biochem-*

istry **34,** 2447–2454
11. Iyer, G. H., Garrod, S., Woods, V. L., Jr., and Taylor, S. S. (2005) *J. Mol. Biol.* **351,** 1110–1122
12. Orr, J. W., and Newton, A. C. (1994) *J. Biol. Chem.* **269,** 27715–27718
13. Stempka, L., Girod, A., Müller, H. J., Rincke, G., Marks, F., Gschwendt, M., and Bossemeyer, D. (1997) *J. Biol. Chem.* **272,** 6805–6811
14. Liu, Y., Belkina, N. V., Graham, C., and Shaw, S. (2006) *J. Biol. Chem.* **281,** 12102–12111
15. Komander, D., Kular, G., Deak, M., Alessi, D. R., and van Aalten, D. M. (2005) *J. Biol. Chem.* **280,** 18797–18802
16. Huang, X., Begley, M., Morgenstern, K. A., Gu, Y., Rose, P., Zhao, H., and Zhu, X. (2003) *Structure* **11,** 21–30
17. Lodowski, D. T., Pitcher, J. A., Capel, W. D., Lefkowitz, R. J., and Tesmer, J. J. (2003) *Science* **300,** 1256–1262
18. Cheetham, G. M., Knegtel, R. M., Coll, J. T., Renwick, S. B., Swenson, L., Weber, P., Lippke, J. A., and Austen, D. A. (2002) *J. Biol. Chem.* **277,** 42419–42422
19. Iyer, G. H., Moore, M. J., and Taylor, S. S. (2005) *J. Biol. Chem.* **280,** 8800–8807
20. Cauthron, R. D., Carter, K. B., Liauw, S., and Steinberg, R. A. (1998) *Mol. Cell Biol.* **18,** 1416–1423
21. Cheng, X., Ma, Y., Moore, M., Hemmings, B. A., and Taylor, S. S. (1998) *Proc. Natl. Acad. Sci. U.S.A.* **95,** 9849–9854
22. Pace, C. N. (1986) *Methods Enzymol.* **131,** 266–280
23. Cook, P. F., Neville, M. E., Jr., Vrana, K. E., Hartl, F. T., and Roskoski, R., Jr. (1982) *Biochemistry* **21,** 5794–5799
24. Yang, J., Garrod, S. M., Deal, M. S., Anand, G. S., Woods, V. L., Jr., and Taylor, S. (2005) *J. Mol. Biol.* **346,** 191–201
25. Moore, M. J., Kanter, J. R., Jones, K. C., and Taylor, S. S. (2002) *J. Biol. Chem.* **277,** 47878–47884
26. Akamine, P., Madhusudan, Wu, J., Xuong, N. H., Ten Eyck, L. F., and Taylor, S. S. (2003) *J. Mol. Biol.* **327,** 159–171
27. Humphries, K. M., Deal, M. S., and Taylor, S. S. (2005) *J. Biol. Chem.* **280,** 2750–2758
28. Torkamani, A., Kannan, N., Taylor, S. S., and Schork, N. J. (2008) *Proc. Natl. Acad. Sci. U.S.A.* **105,** 9011–9016
29. Pike, A. C., Rellos, P., Niesen, F. H., Turnbull, A., Oliver, A. W., Parker, S. A., Turk, B. E., Pearl, L. H., and Knapp, S. (2008) *EMBO J.* **27,** 704–714
30. Lee, S. J., Cobb, M. H., and Goldsmith, E. J. (2009) *Protein Sci.* **18,** 304–313
31. Oliver, A. W., Knapp, S., and Pearl, L. H. (2007) *Trends Biochem. Sci.* **32,** 351–356
32. Oliver, A. W., Paul, A., Boxall, K. J., Barrie, S. E., Aherne, G. W., Garrett, M. D., Mittnacht, S., and Pearl, L. H. (2006) *EMBO J.* **25,** 3179–3190
33. Lee, T., Hoofnagle, A. N., Resing, K. A., and Ahn, N. G. (2005) *J. Mol. Biol.* **353,** 600–612
34. Sours, K. M., Kwok, S. C., Rachidi, T., Lee, T., Ring, A., Hoofnagle, A. N., Resing, K. A., and Ahn, N. G. (2008) *J. Mol. Biol.* **379,** 1075–1093